KcsA: It's a Potassium Channel

Meredith LeMasurier, Lise Heginbotham, and Christopher Miller

Department of Biochemistry, Howard Hughes Medical Institute, Brandeis University, Waltham, MA 02454

ABSTRACT Ion conduction and selectivity properties of KcsA, a bacterial ion channel of known structure, were studied in a planar lipid bilayer system at the single-channel level. Selectivity sequences for permeant ions were determined by symmetrical solution conductance ($K^+ > Rb^+$, NH_4^+, $Tl^+ \gg Cs^+$, Na^+, Li^+) and by reversal potentials under bi-ionic or mixed-ion conditions ($Tl^+ > K^+ > Rb^+ > NH_4^+ \gg Na^+$, Li^+). Determination of reversal potentials with submillivolt accuracy shows that K^+ is over 150-fold more permeant than Na^+. Variation of conductance with concentration under symmetrical salt conditions is complex, with at least two ion-binding processes revealing themselves: a high affinity process below 20 mM and a low affinity process over the range 100–1,000 mM. These properties are analogous to those seen in many eukaryotic K^+ channels, and they establish KcsA as a faithful structural model for ion permeation in eukaryotic K^+ channels.

KEY WORDS: ion conductivity • selectivity

INTRODUCTION

Investigations of K^+ channel mechanisms have been marked by functional feast and structural famine. For nearly 50 yr, K^+ channels in eukaryotic cells have been subjected to detailed electrophysiological analysis for two basic purposes: (1) to understand their varied biological roles in ion transport and membrane electrical behavior, and (2) to reveal their underlying molecular characteristics. The electrical properties of K^+ channels have been unusually informative toward both of these ends, and indeed accumulated work from many labs at the purely functional level has led to a remarkably detailed molecular picture of K^+ channels. The high resolution structure of KcsA, a prokaryotic K^+ channel, now provides a direct structural rationale for the functional behaviors long studied in eukaryotic K^+ channels (Doyle et al., 1998). Therefore, it is ironic that the electrophysiological properties of KcsA itself have been only sparsely described, and at rather low functional resolution. To assess the validity of KcsA as a structural reference for permeation and selectivity in the ubiquitous K^+ channel family, a close examination of ion conduction in this bacterial channel is needed.

Two features of eukaryotic K^+ channels are considered universal: (1) high selectivity among monovalent cations and (2) multiple ion occupancy in the pore. These channels permit permeation by K^+, Rb^+, NH_4^+, and Tl^+ (Hille, 2001) while excluding Na^+ by ~1,000-fold (Yellen, 1984; Neyton and Miller, 1988a; Heginbotham and MacKinnon, 1993). For the KcsA structure to be considered mechanistically explanatory for eukaryotic K^+ channels, high selectivity should be observed in this prokaryotic channel as well. However, the few published reports on ion conduction in KcsA offer sharply contradictory views of its pore. On one hand, KcsA channels reconstituted into liposomes showed familiar properties: strong selection for K^+ and Rb^+ over Na^+ and specific block by Ba^{2+} (Cuello et al., 1998; Heginbotham et al., 1998), but these experiments used low resolution radioactive fluxes. In contrast, several direct single-channel studies (Schrempf et al., 1995; Meuser et al., 1999; Splitt et al., 2000) reported robust conduction by Na^+, Li^+, and Mg^{2+} along with K^+, a characteristic never described for any eukaryotic K^+ channel. These reports led to three alarming conclusions: (1) that in its conducting conformation, the permeation pathway of KcsA is 6 Å wide at its narrowest point; (2) that K^+ permeates with a full hydration shell; and (3) that the high resolution structure of KcsA is misleading as a model for ion conduction in K^+ channels.

In this study, we examine ion-permeation properties of KcsA with a classical, high resolution electrophysiological approach. Purified KcsA protein was reconstituted into a chemically defined planar lipid bilayer system, and single-channel properties were observed under varying conditions of ion concentration, ion type, and voltage. We show that KcsA is readily permeable to K^+ and its close analogues Rb^+, NH_4^+, and Tl^+, whereas permeability for Na^+, Li^+, and Cs^+ is undetectable. The experiments show that in its ion-conduction properties KcsA behaves according to familiar principles long established in eukaryotic K^+ channels.

The online version of this article contains supplemental material.

The present address of L. Heginbotham is Department of Molecular Biophysics and Biochemistry, Yale University New Haven, CT 06520.

Address correspondence to Christopher Miller, Department of Biochemistry, Howard Hughes Medical Institute, Brandeis University, Waltham, MA 02454. Fax: (781) 736-2365; E-mail: cmiller@brandeis.edu

MATERIALS AND METHODS

Materials

Chemicals were of reagent grade or higher. High purity KCl (99.999%), NaCl (99.5%), LiCl (99%), CsCl (>99.5%), RbCl (99+%), $TlNO_3$ (99.999%), Tl(I) acetate (99.99%), and NH_4Cl (99.99%) were obtained from Sigma-Aldrich. Dodecylmaltoside was purchased from Calbiochem, and Chaps was purchased from Pierce Chemical Co. Lipids (Avanti Polar Lipids) were 1-palmitoyl-2-oleoyl phosphatidylethanolamine (POPE) and phophatidylglycerol (POPG) stored in sealed ampules at −80°C.

Solutions used for planar bilayer recording contained the desired salt and an appropriate anionic buffer at a concentration of 10 mM: HEPES for pH 7.0 and succinate for pH 4. Internal and external solutions were adjusted to pH 4.0 and pH 7, respectively, with calibrated solutions of hydroxides of the appropriate cations; this pH gradient is used to eliminate activity of channels inserted "backward" into the bilayer (Heginbotham et al., 1999). The major anion used in most cases was Cl^-, with the exception of the Tl^+ solutions, which necessitated the use of NO_3^-or CH_3COO^-. Replacing Cl^- with these anions has no effect on channel properties. In Tl^+ solutions, *N*-methylglucamine base (NMG) was used for external pH adjustment. The Axopatch 200A amplifier was connected to the recording solutions via KCl salt bridges containing 2% LE agarose and 5 mM K-EGTA.

Purification and Reconstitution of KcsA

The KcsA construct, under control of a tetracycline promoter (model pASK-IBA2; Sigma-Genosys), was as described previously (Heginbotham et al., 1997) except that the strep tag and the two nonnative amino acids appended to the COOH terminus were removed. Thus, the construct carries an NH_2-terminal hexahistidine tag followed by the native sequence of the protein. We found that KcsA conductance is weakly sensitive to the position of the His-tag, with the NH_2-terminal construct having a chord conductance ~25% lower than that of COOH-terminal construct. The overall shapes of the I-V curve and of the K^+ conductance-concentration curve are identical for these two variants.

KcsA was expressed at 37°C in *Escherichia coli* (strain JM-83) and purified in 1 mM dodecylmaltoside as described previously (Heginbotham et al., 1997). Immediately after purification, KcsA was mixed with lipids solubilized in 34 mM Chaps (7.5 mg/ml POPE − 2.5 mg/ml POPG) at 0.4–1 μg protein/mg lipid (Heginbotham et al., 1999). The micellar mixture (0.5 ml) was run over a 20-ml Sephadex G-50 column to form KcsA-reconstituted liposomes, which were stored in aliquots at −80°C for no longer than 3 mo.

Single-channel Recording and Criteria for Channel Analysis

The horizontal planar bilayer system (Chen and Miller, 1996; Heginbotham et al., 1999) consisted of two aqueous chambers separated by a partition crafted from overhead-transparency film 80 μm in thickness. Holes 50–90 μm in diameter were formed by poking the film with butterfly-mounting pins (Elephant-type; Ianni Butterfly Enterprises), and then shaving the nippled surface smooth with a razor blade. Bilayer capacitances were in the range 25–40 pF. Partitions were pretreated by applying ~0.5 μL of lipid solution (7.5 mg/ml POPE + 2.5 mg/ml POPG in n-decane) to the hole and drying in air for 20 min. The chambers were then filled with solution, and bilayers were formed by "painting" the hole with a glass rod dipped in the lipid solution. Channels were inserted by adding ~1 μl of KcsA-containing liposomes over the hole and painting a new bilayer. Typically, several channels were incorporated, but because of the channel's low open probability and long-lived closed intervals, it was straightforward to record stretches of data containing only single-channel openings. The recording system was oriented such that the upper chamber containing pH 7.0 solutions was equivalent to the extracellular side of the channel, and the lower chamber containing pH 4.0 solutions acted as the intracellular solution. Voltages and currents are reported according to electrophysiological convention, with the extracellular solution defined as zero voltage. Current was sampled at 10–50 kHz and low-pass fil-

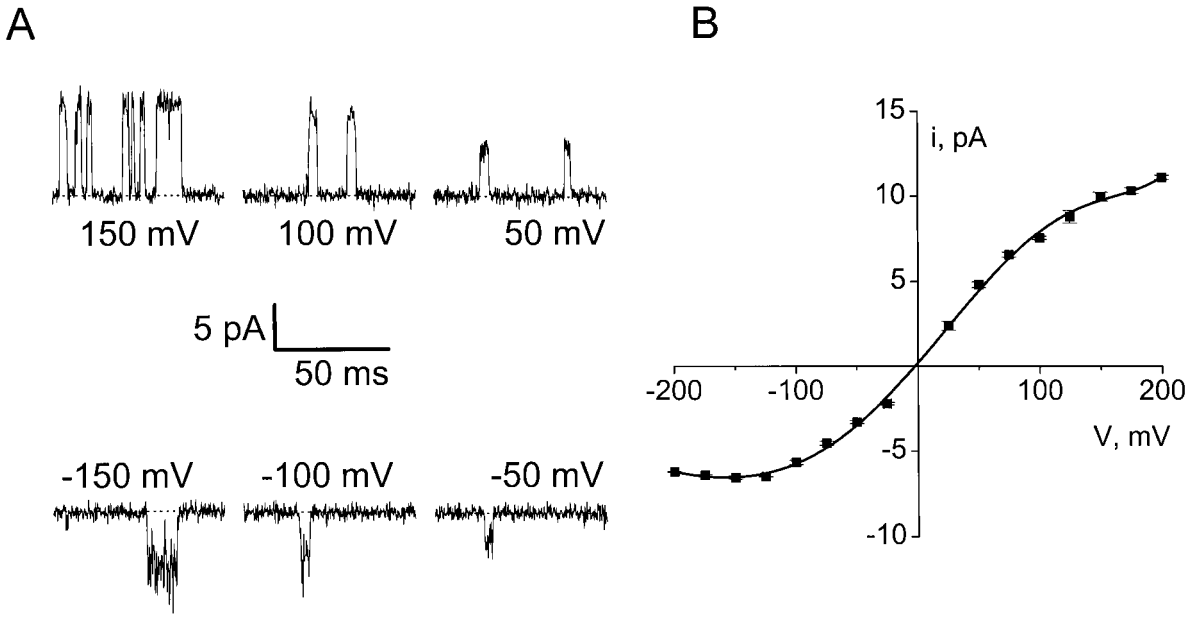

FIGURE 1. Single-channel currents through KcsA. (A) Recordings are shown of single KcsA channels in symmetrical 100 mM KCl at the voltages indicated. The closed state is indicated by dashed lines. (B) Open-channel current-voltage relation. Mean ± standard deviations are shown; standard errors are smaller than the width of the points. Solid curve has no theoretical meaning.

tered at 2–10 kHz, depending on the requirements of the experiment. Most analysis was performed on raw data, but in certain cases, digital filtering (Gaussian, 0.25–1 kHz) was used to resolve low amplitude openings. Typically, single-channel current values report the mean of 30–100 individual measurements taken from at least three separate bilayers. Zero-voltage conductances were calculated from the linear coefficients of fifth-order polynomial fits of the I-V curves. Under bi-ionic or mixed-ionic conditions, permeability ratios (with K^+ as reference ion) were conventionally defined from the measured reversal potential V_r:

$$\exp\left(-\frac{FV_R}{RT}\right) = \frac{[K^+]_{in} + \frac{P_X}{P_K}[X^+]_{in}}{[K^+]_{ex} + \frac{P_X}{P_K}[X^+]_{ex}}. \quad (1)$$

This definition is only useful for reporting permeability ratios, but carries no meaning beyond the raw reversal potential values.

A common hazard of single-channel analysis arises from the extreme sensitivity of the technique and the inherently anecdotal character of the raw recordings. Therefore it is imperative to establish criteria demonstrating that a given experimental record actually represents the channel protein intended for study—rather than denatured protein, peptide fragments, residual detergent, lipid components, or other minor contaminants, all of which produce channel-like activities (Shamoo, 1978; Abramson and Shamoo, 1979; Woodbury, 1989; Grove et al., 1991). This problem is all the more severe in the present case, where there is no established cell-physiological behavior to guide us in identifying a given channel record as arising from properly folded KcsA protein; and the peril is greater still in the ion selectivity studies here, where we apply novel ionic conditions that profoundly alter both conductance and gating. For these reasons, we previously invested considerable effort to establish a "molecular personality" reflecting both conductance and gating behavior of KcsA that allows swift and unambiguous identification of these single channels in K^+ solutions (Heginbotham et al., 1999). Accordingly, in experiments with changed ionic conditions, we first incorporated channels in 100 mM K^+, and only after identifying the current fluctuations as KcsA did we introduce the new solution conditions in the same bilayer. Without these precautions, we would have misidentified a variety of artifactual canaliform current fluctuations as KcsA.

Supplemental Material

Supplemental I-V curve data are available at http:www.jgp.org/cgi/content/full/118/3/303/DC1.

RESULTS

Permeation by K^+

Single-channel current traces for KcsA in symmetrical 100-mM K^+ solutions are illustrated in Fig. 1 A. The voltage- and pH-dependent gating of this channel is complicated (Heginbotham et al., 1999), and all records shown here are representative only of rapid gating within "bursts" of activity, which are interspersed with frequent, long-lived silent periods. The open-channel current-voltage (I-V) curve shows mild outward rectification (Fig. 1 B), with chord conductances of 56 pS and 31 pS for 200 and −200 mV, respectively, and zero-voltage conductance of 97 pS. As with most single channels, open-channel current of KcsA is accompanied by excess noise, as if the channel undergoes rapid unresolved fluctuations, an effect particularly severe at negative potentials. We have therefore confined our analysis to data at positive voltages. At high positive potentials, the I-V curve hints at leveling off. This effect is unlikely to reflect rapid block by contaminating multivalent cations in the internal solution, since we observe identical I-V curves using reagent-grade or ultra-pure KCl, different types of pH buffers, or solutions containing 50 μM Ca^{2+}. (This idea cannot be tested in the obvious way, by addition of chelators like EDTA, since the internal solution must be kept near pH 4.) It is also unlikely that this represents proton block, since the I-V curve is unaffected within ±6% by pH in the range 3.8–4.7 or by a fivefold increase in succinate buffer concentration at fixed pH.

Fig. 2 A shows representative single-channel openings for KcsA in the presence of different symmetrical concentrations of K^+. Not only does the current amplitude increase with K^+ concentration, but open times and open probability greatly decrease as K^+ increases, an effect localized to the intracellular side of the membrane. Amplitude histograms (from data taken exclusively within single-channel bursts and therefore not reflective of overall open probability) show well-defined peaks devoid of "subconductances." A series of I-V curves at different concentrations of K^+ is shown in Fig. 2 B. Outward rectification decreases as K^+ concentration is lowered, such that at 20 mM K^+, the I-V curve is nearly symmetrical.

KcsA conductance increases in a sublinear fashion with symmetrical K^+ concentration over the range 5–1,600 mM, as shown in Fig. 3 for both zero-voltage slope conductance and 200-mV chord conductance. Although the absolute values differ, the shapes of the conductance-concentration curves are identical for the two conductance measurements. The conductance increases with concentration in two stages, a low concentration "burst" phase (0–20 mM) followed by a much slower "creep" in conductance that fails to reach full saturation even at 1,600 mM K^+. The curve shows that the lower limit for half-saturation of the conductance lies above 450 mM K^+. As expected for multi-ion single-file channels, the conductance-concentration curve cannot be even crudely fit by a rectangular hyperbola (demanded of a simple single-ion conduction mechanism) or by a linear function (demanded of an independent, constant-field electrodiffusion mechanism).

Conduction by K^+ Analogues

To assess ion selectivity under symmetrical solution conditions, we first recorded KcsA channels in K^+ solutions, and then perfused both sides of the bilayer with solutions of each of six different monovalent cations at 100 mM: Rb^+, Tl^+, NH_4^+, Li^+, Na^+, and Cs^+. Single-channel

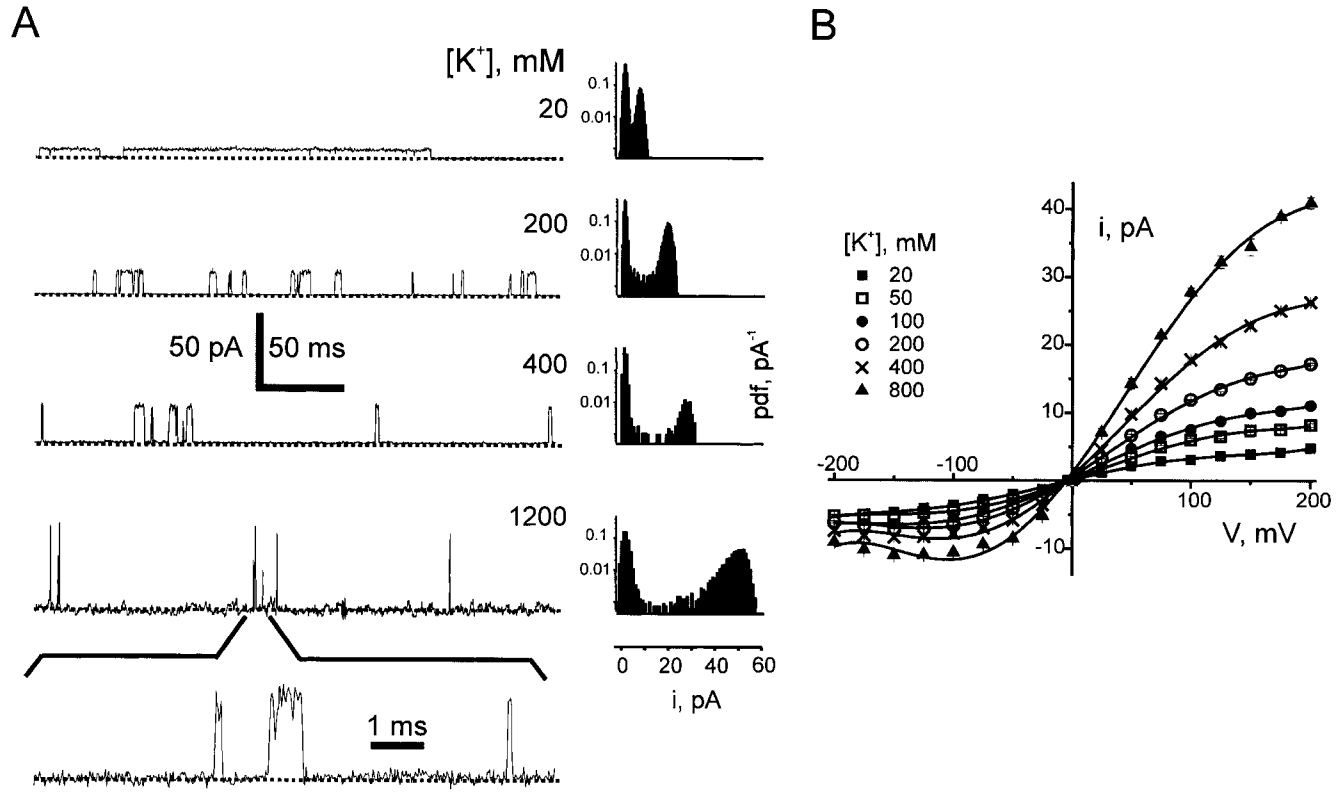

FIGURE 2. KcsA currents in varying concentrations of K^+. Currents were recorded in symmetrical K^+ solutions at the concentrations indicated, at a holding potential of 200 mV. (A) Representative single-channel openings accompanied by amplitude histograms (calculated as probability density, pdf) taken on 0.7–15 s data blocks from which long-lived closed intervals were excluded. Recordings were filtered at 2 kHz, except for the trace at 1,200 mM K^+, which was recorded at 10 kHz filtering; this record is displayed with 2 kHz digital filtering and in the expanded timescale at 10 kHz to show full-amplitude openings. (B) I-V curves at K+ concentrations are indicated. Solid lines are polynomial fits for the determination of the zero-voltage conductance. Above 800 mM K+, open probability becomes so low that full I-V curves could not be measured.

fluctuations were detected for only the first three of these, in addition to K^+ itself (Fig. 4 A). The channels' gating characteristics are strikingly dependent on the

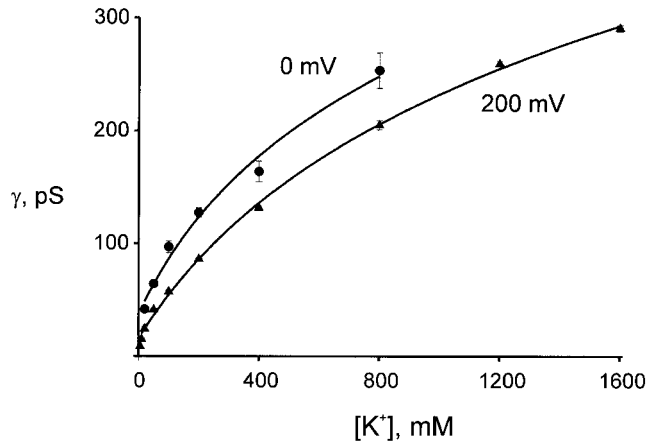

FIGURE 3. Conductance-concentration curve for KcsA in K^+. Conductance of KcsA in symmetrical K^+ solutions was determined in two ways: by the zero-voltage slope conductance (circles) and from 200 mV chord conductance (triangles). Solid lines have no theoretical meaning.

conducting ion (e.g., note long open-times in Rb^+ and NH_4^+), and open-channel amplitudes are well-defined in all cases. As with K^+ (Heginbotham et al., 1999), conductance-substates are not apparent. (In Rb^+ solutions, we observe rare and short-lived excursions to a higher conductance level apparently associated with KcsA; we have not characterized these brief sojourns, which account for <0.1% of the channel record.) The 200-mV chord-conductance is highest for K^+ (56 pS), followed by NH_4^+ (24 pS), Rb^+ (23 pS), and Tl^+ (16 pS). A slightly different selectivity sequence is followed by the zero-voltage conductance determined from the current-voltage relationships (Fig. 4 B): K^+ (97 pS) > Tl^+ (42 pS) > NH_4^+ (15 pS) > Rb^+ (7 pS). KcsA is a weak outward rectifier in all four permeant ions, and the detailed shape of the I-V curve differs for each. Most notably, the I-V curve for Rb^+ remains superlinear over the entire voltage range, and Tl^+ current becomes conspicuously voltage-independent above 100 mV; this maximum level of Tl^+ current cannot reflect diffusion limitation, since its value lies far below that of K^+ current at high voltages, whereas the aqueous diffusion coefficients of Tl^+ and K^+ are essentially identical.

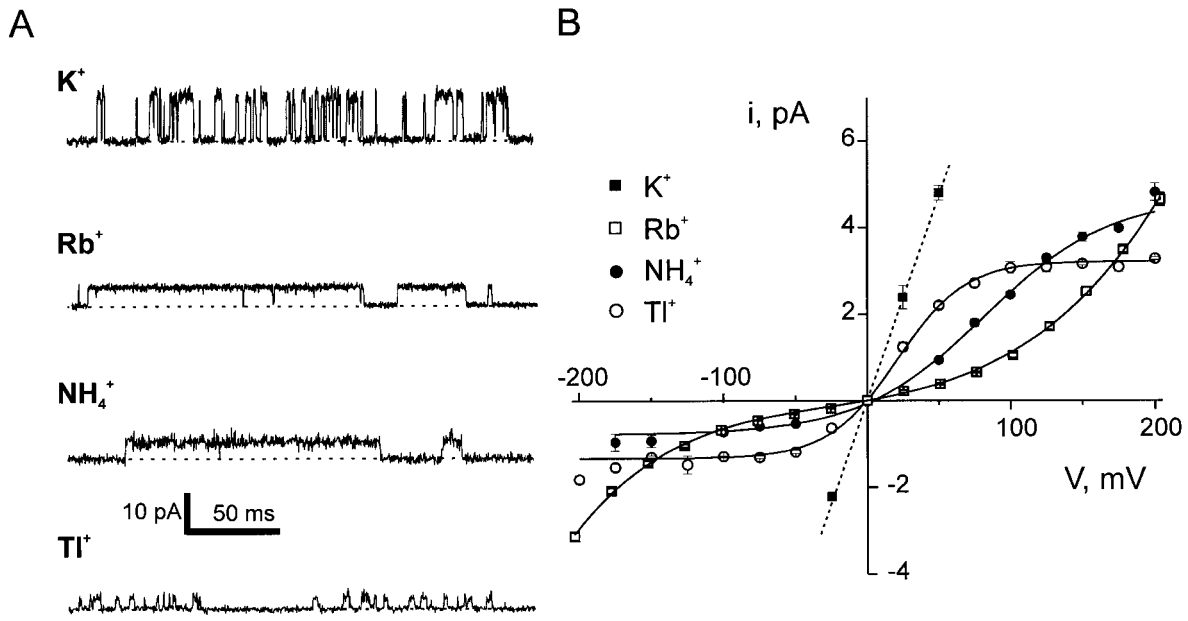

FIGURE 4. Selectivity of KcsA: permeant ions under symmetrical conditions. Channels were recorded in 100 mM symmetrical solutions of the ions indicated. (A) Representative single-channel openings at 200 mV. (B) Single-channel I-V curves, as in Fig 1. Dashed curve compares I-V relation for K^+, as in Fig. 1 B.

Conductance-concentration curves for all permeant ions are plotted in Fig. 5, displayed for clarity on two different scales. As with K^+, the curves have bimodal shapes, with a low concentration increase in conductance followed by a creep, which is far more prominent for K^+ than for the other ions. For the K^+ analogues, half-saturation concentrations are ~90 mM for Rb^+, 120 mM for NH_4^+, and 45 mM for Tl^+, as if all three bind ~5–10-fold more strongly than does K^+.

Selectivity under Bi-ionic Conditions

Ionic selectivity of KcsA was further assessed by observing channels under bi-ionic conditions, i.e., with K^+ in the external solution and an equal concentration of test cation in the internal. Fig. 6 displays traces in which voltage was increased linearly from −200 to 200 mV over 1 s; in these "voltage-ramp" experiments, 100 sweeps were accumulated in each set of ionic condi-

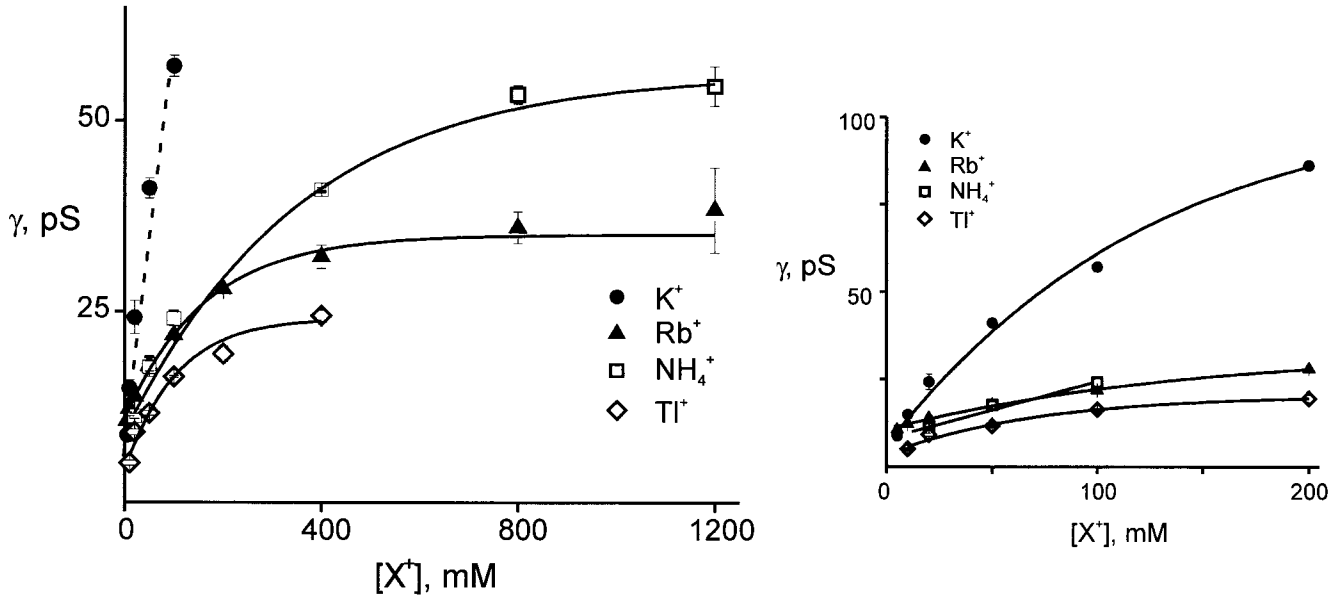

FIGURE 5. Conductance-concentration curves for permeant ions. KcsA conductance at 200 mV was measured with symmetrical solutions of the indicated concentrations of Tl^+, NH_4^+, and Rb^+, as for K^+ in Fig. 2. For clarity, data are shown at two different concentration and conductance scales.

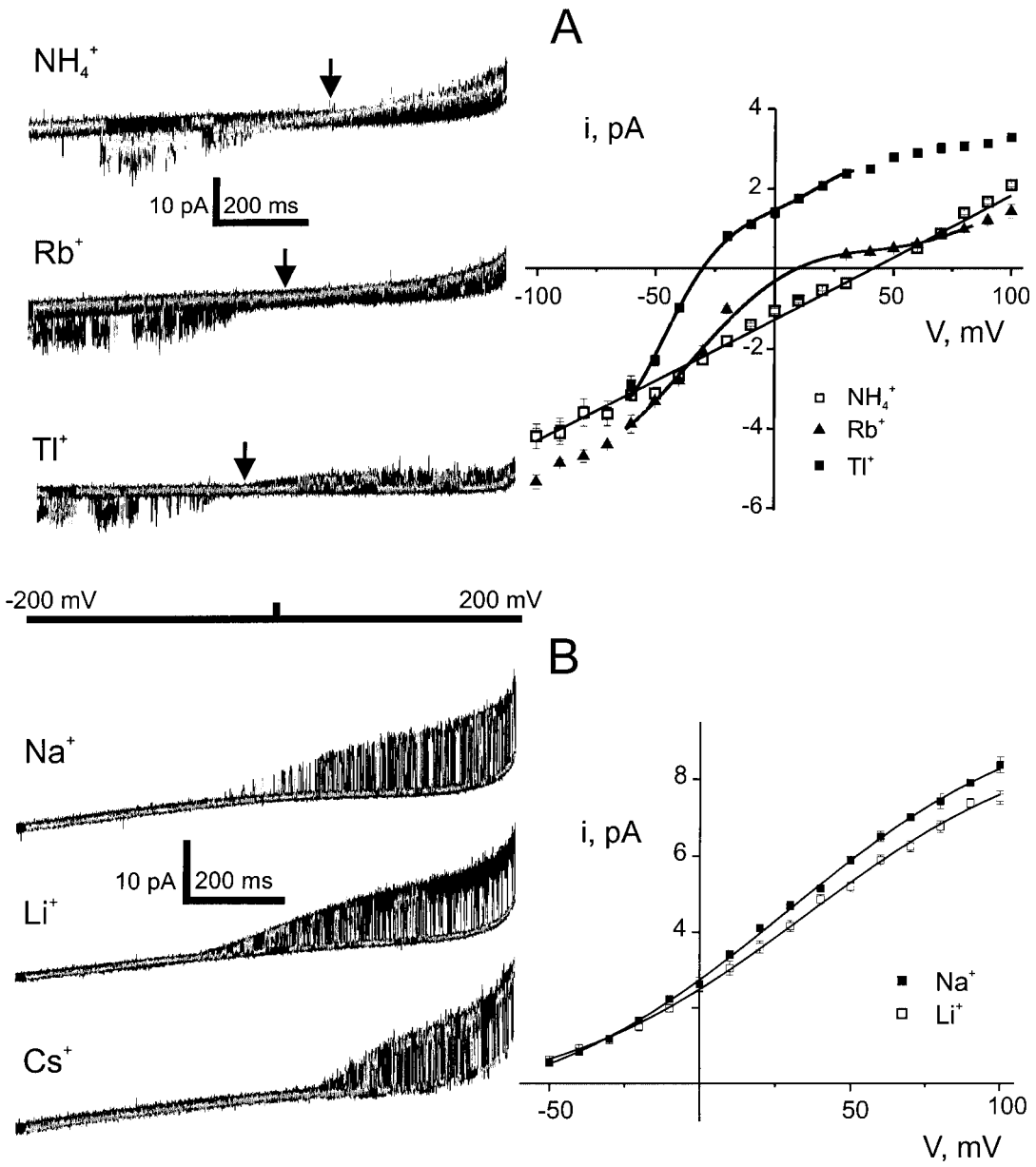

FIGURE 6. KcsA selectivity under bi-ionic conditions. Currents from KcsA were recorded with 100 mM K^+ on the extracellular side and 100 mM of the indicated test cation on the intracellular side. For each data set, 100 voltage-ramps (–200 mV to 200 mV over 1 s) were accumulated; for ease of viewing, only a subset for each trial is shown, and an individual ramp is highlighted in gray (left). Arrows indicate reversal potentials separately determined from I-V curves (right) measured under identical ionic conditions at constant holding voltages. Junction potential corrections were less than 2 mV for permeant ions. (A) Permeant ions. (B) Impermeant ions.

tions, and a single representative sweep is highlighted in the figure. Reversal potentials determined from I-V curves measured at constant holding voltages are indicated by arrows. According to electrophysiological convention (Eq. 1), we define permeability ratios from these measured reversal potentials: $Tl^+(3.2) > K^+(1) > Rb^+(0.8) > NH_4^+(0.2)$. Thus, all conductive ions (Fig. 6 A) show substantial bi-ionic permeability, and under these ionic conditions the least conductive ion, Tl^+, emerges as the most "permeant," a circumstance often associated with tightly binding permeating ions in both cation and anion channels (Urban et al., 1980; Cukierman et al., 1985; Rychkov et al., 1998). A few bi-ionic experiments with reversed orientation gave similar permeability ratios.

Because KcsA currents were not observed in symmetrical solutions of Li^+, Na^+, or Cs^+, these ions were also tested in bi-ionic conditions (Fig. 6 B). In these experiments, we placed K^+ in the internal solution and the test cation in the external, since internal (but not external) Na^+ is a strong voltage-dependent blocker of KcsA (Heginbotham et al., 1999). For all three ions, KcsA

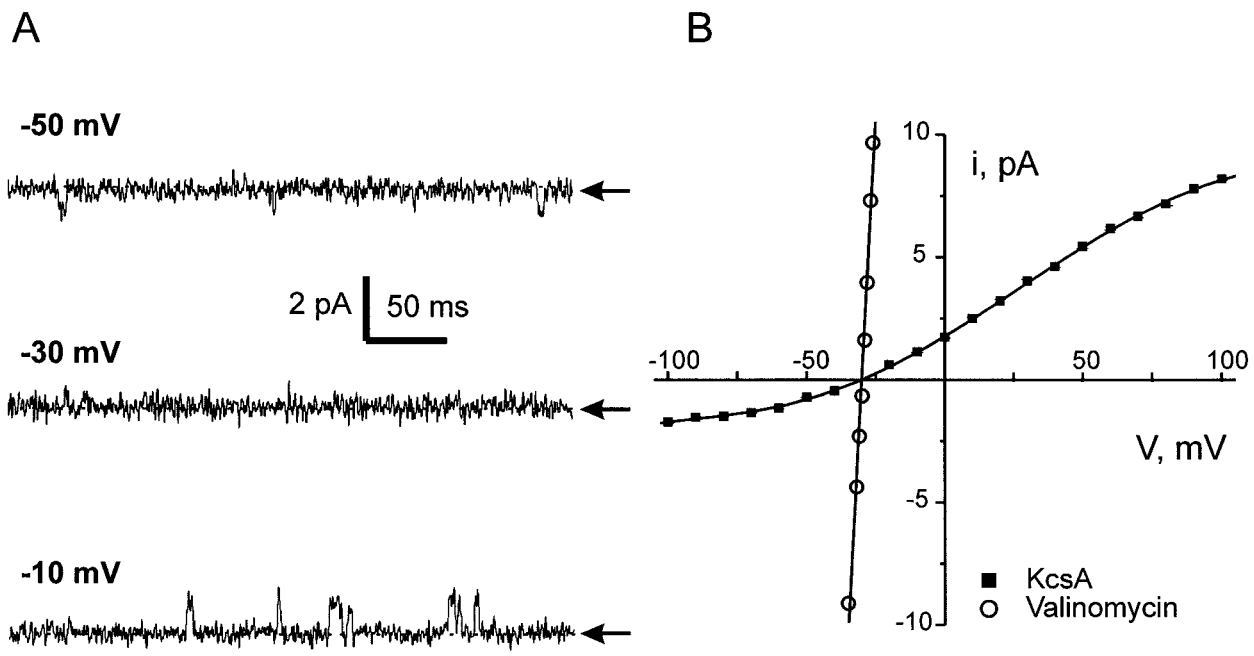

FIGURE 7. Lack of Na^+ permeability under mixed ion conditions. Single-channel recordings were collected with 100 mM K^+ internal and 20 mM K^+ + 100 mM Na^+ external. After recording the channels, valinomycin (10–50 μM) was added to the external solution to produce a large, ideally K^+-selective leak in the planar bilayer, and another I-V curve was taken. Left: illustrative single-channel openings taken on either side of the KcsA reversal potential. Right: I-V curves for KcsA-mediated current (filled points) and valinomycin-mediated current (open points). Average value (± s.e.) of V_r taken from four separate experiments was 180 ± 250 μV.

channels carrying outward K^+ current were readily observed, but current was never seen to reverse to the inward direction, even at voltages as high as −200 mV. For Na^+ and Li^+, clear outward K^+ current was detected at −50 mV, and so the reversal potential for these ions, if it exists at all, is certainly more negative than this. Ramp traces in Cs^+ differ markedly from those in Na^+ or Li^+. In the Cs^+ case, not only do we fail to see outward K^+ current at negative voltages, but outward current falls to zero at positive potentials; in this circumstance, the reversal potential could have any value less than about +30 mV, and so we cannot say whether the Cs^+/K^+ permeability ratio is greater than, equal to, or less than unity. This phenomenon is a reflection of block by external Cs^+, a common observation in many types of K^+ channels (Bezanilla and Armstrong, 1972; Hille, 1973; Hagiwara et al., 1976; Gay and Stanfield, 1977; Adelman and French, 1978; Cecchi et al., 1987).

The absence of Na^+ current in bi-ionic conditions provoked a more sensitive test of Na^+ permeation. Here, in the presence of a K^+ gradient (100 mM internal/20 mM external), we examined the degree to which addition of 100 mM external Na^+ perturbs the K^+-dominated reversal potential. The single-channel I-V curve is shown in Fig. 7, along with raw records near the reversal potential (−30 mV in this experiment). Because of uncertain liquid–junction corrections, unstirred layer effects, and other imbalances, the relation of the measured reversal potential of the recording system to the absolute reversal potential across the planar bilayer is uncertain within ~10 mV. To obtain a more accurate value, as required for our purposes here, we used valinomycin, an ideally K^+-selective ionophore, to determine the true equilibrium potential for K^+ in each experiment, as in previous submillivolt precision measurements of single-channel reversal potentials (Miller, 1982). After recording KcsA channel I-V curves, we added a high concentration of valinomycin to increase the planar bilayer's K^+ conductance ~100-fold, and determined the reversal potential of the valinomycin-mediated current within 200 μV. As shown in Fig. 7, this value is indistinguishable from the KcsA reversal potential. Considering that for valinomycin conductance $P_{Na}/P_K \sim 10^{-4}$ (Eisenman et al., 1973), this experiment dramatically illustrates the low permeability of Na^+ to KcsA. Straightforward analysis shows that for the ionic conditions here, the difference, ΔV_r, between the reversal potentials of valinomycin-mediated and KcsA-mediated currents is:

$$\frac{F\Delta V_r}{RT} = \ln\left(1 + \frac{P_{Na}}{P_K}\frac{[Na^+]_{ex}}{[K^+]_{ex}}\right),$$

which, given the small measured value of ΔV_r, simplifies to:

$$\frac{P_{Na}}{P_K} = \frac{F\Delta V_r}{RT}\frac{[K^+]_{ex}}{[Na^+]_{ex}}.$$

Our value of ΔV_r determined in four independent experiments (180 ± 250 μV) puts a very conservative upper limit on the Na^+/K^+ permeability ratio for KcsA of ~0.006. This upper limit is consistent with measurements in certain eukaryotic K^+ channels that offer opportunities for more precise selectivity determinations (e.g., Yellen, 1984; Neyton and Miller, 1988a,b).

DISCUSSION

It is widely appreciated that ion selectivity of eukaryotic K^+ channels is both biologically necessary and mechanistically informative. These proteins have evolved to pass K^+ efficiently, and at rates ~1,000-fold greater than for Na^+, the physiologically relevant competitor cation. The structure of KcsA, despite its prokaryotic origin, provides a rich model illuminating the mechanism by which K^+ channels achieve rapid permeation along with strong ionic selectivity. Under physiological ionic conditions, KcsA is occupied by up to three K^+ ions constrained to move in single file (Doyle et al., 1998; Jiang and MacKinnon, 2000). Two of these are largely dehydrated and intimately coordinated by carbonyl oxygens in the narrow (3-Å diam) selectivity filter located near the external pore opening, whereas a third ion resides fully hydrated in a wider (10-Å diam), nonselective region near the middle of the pore. This structure provides a unique foundation for interpreting K^+ channel function.

In the ion conduction properties reported here, KcsA is reminiscent of eukaryotic K^+ channels (Table I). At physiological K^+ concentrations, the conductance of KcsA falls solidly within the range of values measured for K_v, K_{ir}, and BK-type channels. Moreover, ions known to permeate eukaryotic K^+ channels also permeate KcsA with a similar selectivity sequence, and those known to be impermeant are excluded from this prokaryotic channel.

Beyond this familiar behavior, several characteristics of KcsA are notable. First, this channel's gating is extraordinarily sensitive to the type and concentration of conducting ion. The classic "foot-in-the-door" mechanism, by which ion occupancy of the pore inhibits closing, is customarily invoked to explain coupling of ion permeation to gating in K^+ channels (Swenson and Armstrong, 1981; Demo and Yellen, 1992). But this mechanism cannot account for the ion-dependent gating seen in KcsA, as is apparent from two observations (Figs. 2 and 4): (1) that channel closing becomes dramatically faster, not slower, with K^+ concentration; and (2) that channel closing rate is not correlated with ion binding affinity (fast in K^+ and Tl^+, slow in Rb^+). At this point, we have no explanation for the influence of ions upon KcsA gating. We emphasize that even with Rb^+, which strongly promotes opening (Fig. 4), long-lived closed states are still present, and overall open probability of the channel remains low (typically below 0.4) under all conditions; therefore, Rb^+ cannot be considered a magic bullet to lodge the channel open.

A second noteworthy feature of KcsA is the common shape of the conductance-concentration curves for all four permeant ions. These curves show two distinct phases: a burst of conductance below 20 mM, and a subsequent creep as concentration increases up to 1 M and above, as has also been observed in mammalian Ca^+-activated K^+ channels (Eisenman et al., 1986). It is striking that K^+, Rb^+, and NH_4^+ produce nearly identical conductances at 5 mM, whereas at high concentrations, these differ by factors of 5–8. These measurements are made at voltages far from equilibrium, and surface-electrostatic effects may influence the shapes of these curves, so it is uncertain to interpret them in terms of ion occupancies in the pore (Coronado and Miller, 1980); nonetheless, more rigorous measurements of equilibrium ion binding to other K^+ channels provide such compelling analogies to our results that a qualitative reading of the KcsA conductance curves is justified. Accordingly, we suggest that the low concen-

TABLE I

Comparison of Selectivity Properties of Several K^+ Channels

	γ, pS				P_x/P_K, bi-ionic		
Channel	K^+	Rb^+	NH_4^+	Tl^+	Rb^+	NH_4^+	Tl^+
KcsA	55.6 ± 0.6	23.2 ± 0.8	24.0 ± 0.3	16.4 ± 0.1	0.78 ± 0.07	0.20 ± 0.01	3.2 ± 0.1
	(97 ± 5)	(7.4 ± 0.7)	(15 ± 1)	(42 ± 1)			
Shaker	18	9	14	–	0.66	0.09	–
BK	230	20	41	111	0.7	0.1	1.3
$K_{ir}2.1$	29	3	17	24	0.49	0.1	1.8

For KcsA, symmetrical solution 200 mV chord-conductance, γ, was measured at 100 mM of the indicated cation; values in parentheses are zero-voltage conductances. Bi-ionic permeability ratios were measured from reversal potentials. Data from other channels (at 100–150 mM K^+) are as follows: *Shaker* from Heginbotham and MacKinnon (1993), BK (high conductance Ca^{2+}-activated K^+ channel from rat skeletal muscle) from Eisenman et al. (1986), and $K_{ir}2.1$. Data from Choe et al. (2000). For KcsA, each value represents mean ± SEM of 50–100 determinations for chord conductance, and three independent measurements for zero-voltage conductance and reversal potential.

tration burst represents occupancy of the KcsA pore by the first two ions, in analogy with Ca^+-activated K^+ channels, where two sites bind K^+ and Rb^+ in the range 3 μM–10 mM (Neyton and Miller, 1988a,b; Vergara et al., 1999). It is likely (Jiang and MacKinnon, 2000) that one of these high affinity sites is located in the wide, nonselective "lake," and one in the selectivity filter. The high concentration creep would then represent the gradual filling of a third, low affinity site located in the KcsA selectivity filter, in analogy with the destabilization of pore blockers (charybdotoxin peptides and Ba^{2+}) at and above physiological K^+ concentrations in eukaryotic K^+ channels (MacKinnon and Miller, 1988; Neyton and Miller, 1988b; Giangiacomo et al., 1992; Park and Miller, 1992; Goldstein and Miller, 1993; Ranganathan et al., 1996). In KcsA, the high concentration creep is of much larger amplitude in K^+ than in Rb^+, as though the pore occupancy is on average higher for K^+, possibly reflecting the channel's evolutionary fine-tuning for rapid passage of K^+ (rather than Rb^+) at physiological ion concentrations. In light of the long-held view based on flux-ratio exponents (Hodgkin and Keynes, 1955; Begenisich and DeWeer, 1980; Spalding et al., 1981; Stampe and Begenisich, 1996; Stampe et al., 1998) that three K^+ ions occupy the pore under physiological conditions, this picture is hardly novel, but merely represents a natural reading of K^+ conduction in a structurally explicit context. Speculations of this kind must await direct tests by quantitative crystallographic measurements of ion occupancy in KcsA, which are now nearing feasibility (Jiang and MacKinnon, 2000).

Another point worth mentioning is our failure to detect Cs^+ conduction through KcsA despite the well-known interactions of Cs^+ with K^+ selectivity filters. In macroscopic measurements, Cs^+ permeation has been observed for eukaryotic K^+ channels (Shapiro and DeCoursey, 1991; Heginbotham and MacKinnon, 1993; Olcese et al., 1997), but this ion's conductance is two orders of magnitude lower than that of K^+, well below detection levels for single-channel recordings. In KcsA, we cannot set a useful limit on Cs^+ permeability in bi-ionic experiments because of the block of outward K^+ currents by external Cs^+, also as observed in many eukaryotic K^+ channels.

Our results conflict with suggestions that the high resolution KcsA structure is inadequate as a basis for understanding K^+ permeation (Meuser et al., 1999; Reusch, 1999; Splitt et al., 2000). These doubts are largely based on claims of substantial permeation of KcsA by Na^+ and Li^+, with P_{Na}/P_K permeability ratios in the range 0.1–0.25, far above our upper limit of 0.006. High values like these imply that inward Na^+ currents must have been observed in those studies at potentials near −50 mV, in direct contradiction to the absence in our bi-ionic experiments of Na^+ current as far out as −200 mV. Our results further clash with the claim by Meuser et al. (1999) that K^+, Rb^+, and Cs^+ are equally permeant in bi-ionic conditions. However, these assertions are impossible to evaluate from the published reports, for two reasons. First, the above studies presented neither primary electrophysiological recordings nor I-V curves to support the tabulated permeability ratios; and second, no precautions were described to exclude artifactual conductance fluctuations from the channel recordings, which were taken in bilayers formed from unpurified soy lipid extracts. Therefore, we suggest that the stark discrepancies between our results and previous claims that KcsA is a low selectivity channel arise from channel-like fluctuations erroneously identified as KcsA in those experiments. This suggestion is corroborated by the wide variation in cation-selective conductances and frequent substates reported in the low selectivity channels, features absent in our recordings of KcsA but known to occur with contaminant-induced conductances in planar lipid bilayers.

Our experiments lead to a simple conclusion: KcsA is a conventional K^+ channel. All ion permeation properties common to eukaryotic K^+ channels are recapitulated in KcsA: conduction by K^+, Rb^+, NH_4^+, and Tl^+, exclusion of Li^+, Na^+, and Cs^+, and complex variation of conductance with concentration, as expected for multi-ion occupancy in the pore (Hille and Schwarz, 1978; Blatz and Magleby, 1984; Eisenman et al., 1986; Cecchi et al., 1987; Wagoner and Oxford, 1987; Shapiro and DeCoursey, 1991; Heginbotham and MacKinnon, 1993; Choe et al., 2000). KcsA also exhibits block by Na^+, Ba^{2+}, and Cs^+ (Heginbotham et al., 1998, 1999), which are three additional conserved behaviors of K^+ channels. Accordingly, we can safely view KcsA as an excellent structural paradigm for ion interactions in eukaryotic K^+ channels.

We are grateful to Dr. C. Nimigean for criticisms on the manuscript, to Dr. Z. Lu for suggestions on the experiments, and Dr. R. Blaustein for unceasing mathematical consultations.

This study was supported by a National Institutes of Health grant GM31768 to C. Miller.

Submitted: 26 June 2001
Revised: 2 August 2001
Accepted: 3 August 2001

REFERENCES

Abramson, J.J., and A.E. Shamoo. 1979. Anionic detergents as divalent cation ionophores across black lipid membranes. *J. Membr. Biol.* 50:241–255.

Adelman, W.J., and R.J. French. 1978. Blocking of the squid axon potassium channel by external caesium ions. *J. Physiol. (Lond.)* 276:13–25.

Begenisich, T.B., and P. DeWeer. 1980. Potassium flux ratio in voltage-clamped squid giant axons. *J. Gen. Physiol.* 76:83–98.

Bezanilla, F., and C.M. Armstrong. 1972. Negative conductance caused by entry of sodium and cesium ions into the potassium

channels of squid axons. *J. Gen. Physiol.* 60:588–608.
Blatz, A., and K. Magleby. 1984. Ion conductance and selectivity of single calcium-activated potassium channels in cultured rat muscle. *J. Gen. Physiol.* 84:1–23.
Cecchi, X., D. Wolff, O. Alvarez, and R. Latorre. 1987. Mechanisms of Cs^+ blockade in a Ca^{2+}-activated K^+ channel from smooth muscle. *Biophys. J.* 52:707–716.
Chen, T-Y., and C. Miller. 1996. Nonequilibrium gating and voltage dependence of the ClC-0 Cl^- channel. *J. Gen. Physiol.* 108:237–250.
Choe, H., H. Sackin, and L.G. Palmer. 2000. Permeation properties of inward-rectifier potassium channels and their molecular determinants. *J. Gen. Physiol.* 115:391–404.
Coronado, R., and C. Miller. 1980. Ionic selectivity, saturation, and block in a K^+-selective channel from sarcoplasmic reticulum. *J. Gen. Physiol.* 76:425–453.
Cuello, L.G., J.G. Romero, D.M. Cortes, and E. Perozo. 1998. pH-dependent gating in the *Streptomyces lividans* K^+ channel. *Biochemistry.* 37:3229–3236.
Cukierman, S., G. Yellen, and C. Miller. 1985. The sarcoplasmic reticulum K^+ channel: a new look at Cs^+ block. *Biophys. J.* 48:477–484.
Demo, S.D., and G. Yellen. 1992. Ion effects on gating of the Ca^{2+}-activated K^+ channel correlate with occupancy of the pore. *Biophys. J.* 61:639–648.
Doyle, D.A., J.M. Cabral, A. Pfuetzner, J.M. Kuo, J.M. Gulbis, S.L. Cohen, B.T. Chait, and R. MacKinnon. 1998. The structure of the potassium channel: molecular basis of K^+ conduction and selectivity. *Science.* 280:69–76.
Eisenman, G., G. Szabo, S.G.A. McLaughlin, and S.M. Ciani. 1973. Molecular basis for the action of macrocyclic carriers on passive ionic translocation across lipid bilayer membranes. *Bioenergetics.* 4:93–148.
Eisenman, G., R. Latorre, and C. Miller. 1986. Multi-ion conduction in the high-conductance Ca^{2+}-activated K^+ channel from skeletal muscle. *Biophys. J.* 50:1025–1034.
Gay, L.A., and P.R. Stanfield. 1977. Cs^+ causes a voltage-dependent block of inward K^+ currents in resting skeletal muscle fibres. *Nature.* 267:169–170.
Giangiacomo, K.M., M.L. Garcia, and O.B. McManus. 1992. Mechanism of iberiatoxin block of the large-conductance calcium-activated potassium channel from bovine aortic smooth muscle. *Biochemistry.* 31:6719–6727.
Goldstein, S.A.N., and C. Miller. 1993. Mechanism of charybdotoxin block of a *Shaker* K^+ channel. *Biophys. J.* 65:1613–1619.
Grove, A., J.M. Tomich, and M. Montal. 1991. A molecular blueprint for the pore-forming structure of voltage-gated calcium channels. *Proc. Natl. Acad. Sci. USA.* 64:18–22.
Hagiwara, S., S. Miyazaki, and N.P. Rosenthal. 1976. Potassium current and the effect of cesium on this current during anomalous rectification of the egg cell membrane of a starfish. *J. Gen. Physiol.* 67:621–638.
Heginbotham, L., and R. MacKinnon. 1993. Conduction properties of the cloned *Shaker* channel. *Biophys. J.* 65:2089–2096.
Heginbotham, L., E. Odessey, and C. Miller. 1997. Tetrameric stoichiometry of a prokaryotic K^+ channel. *Biochemistry.* 36:10335–10342.
Heginbotham, L., L. Kolmakova-Partensky, and C. Miller. 1998. Functional reconstitution of a prokaryotic K^+ channel. *J. Gen. Physiol.* 111:741–750.
Heginbotham, L., M. LeMasurier, L. Kolmakova-Partensky, and C. Miller. 1999. Single K^+ channels from *Streptomyces lividans:* functional asymmetries and sidedness of proton activation. *J. Gen. Physiol.* 114:551–560.
Hille, B. 1973. Potassium channels in myelinated nerve. Selective permeability to small cations. *J. Gen. Physiol.* 61:669–686.
Hille, B. 2001. Ionic Channels of Excitable Membranes. 3rd ed. Sinauer Associates, Inc., Sunderland, MA. 814 pp.
Hille, B., and W. Schwarz. 1978. Potassium channels as multi-ion single-file pores. *J. Gen. Physiol.* 72:409–442.
Hodgkin, A.L., and R.D. Keynes. 1955. The potassium permeability of a giant nerve fibre. *J. Physiol.* 128:61–88.
Jiang, Y., and R. MacKinnon. 2000. The barium site in a potassium channel X-ray crystallography. *J. Gen. Physiol.* 115:269–272.
MacKinnon, R., and C. Miller. 1988. Mechanism of charybdotoxin inhibition of Ca^{2+}-activated K^+ channels. *J. Gen. Physiol.* 91:335–349.
Meuser, D., H. Splitt, R. Wagner, and H. Schrempf. 1999. Exploring the open pore of the potassium channel from *Streptomyces lividans. FEBS Lett.* 462:447–452.
Miller, C. 1982. Coupling of water and ion fluxes in a K^+-selective channel of sarcoplasmic reticulum. *Biophys. J.* 38:227–230.
Neyton, J., and C. Miller. 1988a. Discrete Ba^{2+} block as a probe of ion occupancy and pore structure in the high conductance Ca^{2+}-activated K^+ channel. *J. Gen. Physiol.* 92:569–586.
Neyton, J., and C. Miller. 1988b. Potassium blocks barium permeation through calcium-activated potassium channels. *J. Gen. Physiol.* 92:549–567.
Olcese, R., R. Latorre, L. Toro, F. Bezanilla, and E. Stefani. 1997. Correlation between charge movement and ionic current during slow inactivation in *Shaker* K^+ channels. *J. Gen. Physiol.* 110:579–589.
Park, C.S., and C. Miller. 1992. Interaction of charybdotoxin with permeant ions inside the pore of a K^+ channel. *Neuron.* 9:307–313.
Ranganathan, R., J.H. Lewis, and R. MacKinnon. 1996. Spatial localization of the K^+ channel selectivity filter by mutant cycle-based structure analysis. *Neuron.* 16:131–139.
Reusch, R.N. 1999. *Streptomyces lividans* potassium channel contains poly-(R)-3-hydroxybutyrate and inorganic polyphosphate. *Biochemistry.* 38:15666–15672.
Rychkov, G.Y., M. Pusch, M.L. Roberts, T.J. Jentsch, and A.H. Bretag. 1998. Permeation and block of the skeletal muscle chloride channel ClC-1 by foreign anions. *J. Gen. Physiol.* 111:653–665.
Schrempf, H., O. Schmidt, R. Kummerlin, S. Hinnah, D. Muller, M. Betzler, T. Steinkamp, and R. Wagner. 1995. A prokaryotic potassium ion channel with two predicted transmembrane segments from *Streptomyces lividans. EMBO J.* 14:5170–5178.
Shamoo, A.E. 1978. Ionophorous properties of the 20,000-dalton fragment of (Ca^{2+} + Mg^{2+})-ATPase in phosphatidylcholine: cholesterol membranes. *J. Membr. Biol.* 43:227–242.
Shapiro, M.S., and T.E. DeCoursey. 1991. Selectivity and gating of the type L potassium channel in mouse lymphocytes. *J. Gen. Physiol.* 97:1227–1250.
Spalding, B.C., O. Senyk, J.G. Swift, and P. Horowicz. 1981. Unidirectional flux ratio of potassium ions in depolarized frog skeletal muscle. *Am. J. Physiol.* 241:c68–c75.
Splitt, H., D. Meuser, I. Borovok, M. Betzler, and H. Schrempf. 2000. Pore mutations affecting tetrameric assembly and functioning of the potassium channel KcsA from *Streptomyces lividans. FEBS Lett.* 472:83–87.
Stampe, P., and T. Begenisich. 1996. Unidirectional K^+ fluxes through recombinant *Shaker* potassium channels expressed in single *Xenopus* oocytes. *J. Gen. Physiol.* 107:449–457.
Stampe, P., J. Arreola, P. Perez-Cornejo, and T. Begenisich. 1998. Nonindependent K^+ movement through the pore in IRK1 potassium channels. *J. Gen. Physiol.* 112:475–484.
Swenson, R.P., and C.M. Armstrong. 1981. K^+ channels close more slowly in the presence of external K^+ and Rb^+. *Nature.* 291:427–429.
Urban, B.W., S.B. Hladky, and D.A. Haydon. 1980. Ion movements in gramicidin pores. An example of single-file transport. *Biochim. Biophys. Acta.* 602:331–354.
Vergara, C., O. Alvarez, and R. Latorre. 1999. Localization of the

K^+ lock-in and the Ba^{2+} binding sites in a voltage-gated calcium-modulated channel. Implications for survival of K^+ permeability. *J. Gen. Physiol.* 114:365–376.

Wagoner, P.K., and G.S. Oxford. 1987. Cation permeation through the voltage-dependent potassium channel in the squid axon. Characteristics and mechanisms. *J. Gen. Physiol.* 90:261–290.

Woodbury, D.J. 1989. Pure lipid vesicles can induce channel-like conductances in planar bilayers. *J. Membr. Biol.* 109:145–150.

Yellen, G. 1984. Ionic permeation and blockade in Ca^{2+}-activated K^+ channels of bovine chromaffin cells. *J. Gen. Physiol.* 84:157–186.